JACS
JOURNAL OF THE AMERICAN CHEMICAL SOCIETY
pubs.acs.org/JACS
Communication

Reversible-Addition Fragmentation Chain Transfer Step-Growth Polymerization

Joji Tanaka,* Noel Edward Archer, Michael Jeffery Grant, and Wei You*

Cite This: J. Am. Chem. Soc. 2021, 143, 15918−15923
Read Online
ACCESS | Metrics & More | Article Recommendations | Supporting Information

ABSTRACT: Reversible-addition fragmentation chain transfer (RAFT) polymerization has been widely explored since its discovery due to its structural precision, versatility, and efficiency. However, the lack of tunability of the polymer backbone limits some applications. Herein, we synergistically combine RAFT and step-growth polymerization mechanisms, by employing a highly selective insertion process of a single monomer with a RAFT agent, to achieve RAFT step-growth polymerization. A unique feature of the RAFT step-growth polymers is that each backbone repeat unit bears a pendant RAFT agent, which can subsequently graft side chains in a second polymerization step and afford molecular brush polymers. Enabled by cleavable backbone functionality, we demonstrate transformation of the resulting brushlike polymers into linear chains of uniform size upon a stimulus.

Controlled radical polymerization (CRP) has been widely used in creating a plethora of soft functional materials for a broad range of applications from commodities to drug delivery.[1,2] Among many CRP methods, reversible-addition fragmentation chain transfer (RAFT) polymerization[3] stands out as a user-friendly approach that is applicable for a diverse range of monomer families with a variety of side chain functionalities.[4,5] However, inherent to the chain-growth nature of RAFT polymerization, backbones of such polymers usually consist of inert carbon atoms (e.g., C−C bond), limiting applications where degradable functionality is crucial such as in tissue engineering and plastics recycling.[6,7] By contrast, step-growth polymerization can readily incorporate desirable functionalities (e.g., ester for degradation) along the polymer backbone. However, typical strategies for step-growth are limited by low functional group tolerance and harsh reaction conditions.[8]

The RAFT process is mediated by chain transfer agents (CTAs)[9] that seed chain-growth polymerization through the R-group[10,11] and govern the chain transfer exchange via an intermediate.[12] Depending on the reactivity of the CTA and monomer employed, during the initial stages of the RAFT process, the CTA can be preferentially consumed fully, yielding single monomer unit inserted (SUMI) CTA adducts prior to further chain-growth.[13] McLeary and Klumperman were the first to study this unique SUMI process in detail.[13−15] Later, Moad investigated high yielding SUMI-CTA adducts with stoichiometrically balanced monomer and CTA pairs.[16−18] Similarly, Zard had demonstrated iterative insertion of less activated monomers as a divergent method to design complex structures.[19] More recently, Xu expanded the scope of sequence defined polymers via iterative RAFT-SUMI cycles by a photoinduced energy/electron transfer (PET)-RAFT process.[20−24]

We envisioned a highly efficient RAFT-SUMI process could be harnessed using bifunctional reagents of CTA and monomer to permit step-growth polymerization. This new RAFT step-growth polymerization would inherit key benefits from both RAFT (e.g., functional group tolerance and user-friendly nature) and step-growth (e.g., functional backbone) (Scheme 1). In previous reports, the use of such bifunctional reagents (monomer bearing active CTA) has been employed to design hyperbranched polymers;[25] by contrast, in our case, homopropagation of the monomer is suppressed such that a

Scheme 1. Traditional RAFT Polymerization vs RAFT Step-Growth

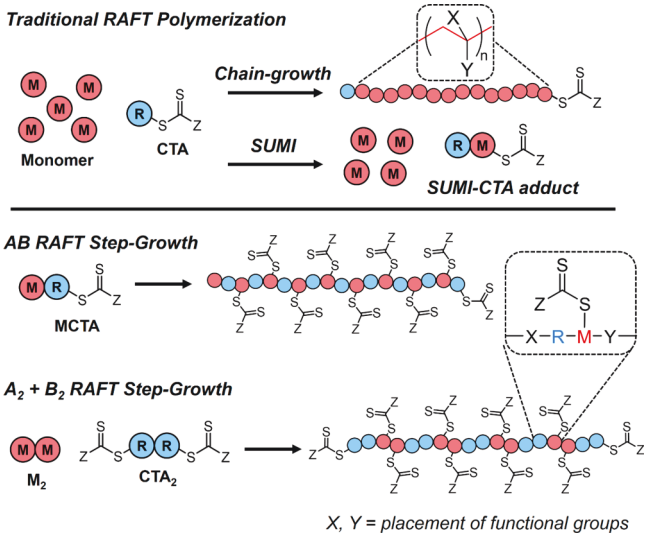

Received: July 20, 2021
Published: September 28, 2021

https://doi.org/10.1021/jacs.1c07553
J. Am. Chem. Soc. 2021, 143, 15918−15923

linear step-growth backbone is obtained via a chain transfer cycle mechanism (iv, Scheme 2). This cycle is driven when the

Scheme 2. Proposed RAFT Step-Growth Mechanism[a]

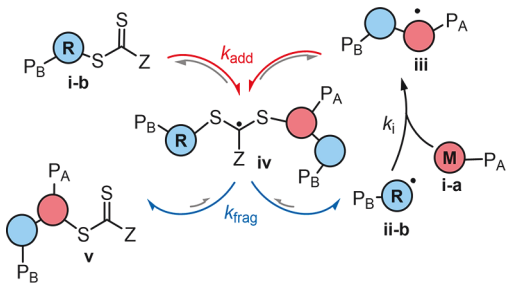

[a]The RAFT step-growth mechanism proceeds through cycle of the radical addition (k_i) between the two end group species: monomer (i-a) and R• (ii-b), forming the backbone radical (iii), followed by chain transfer with the CTA (i-b) end group through reversible addition (k_{add}) and fragmentation (k_{frag}) of the intermediate (iv), to regenerate the R• (ii-b) species and yield the polymer backbone (v).

chain transfer of the monomer radical species (iii) with the CTA (i-b) is significantly more rapid than addition with another monomer and equilibrium of the chain transfer (iv) favoring the formation of R• species (ii-b).[26] In addition, this process is facilitated by rapid monomer (i-a) addition (k_i) to the R• species (ii-b).[26]

We commenced the study by pairing a monomer and a CTA functional group that can selectively form a SUMI-CTA adduct at quantitative yield (Figure 1). We selected *N*-substituted

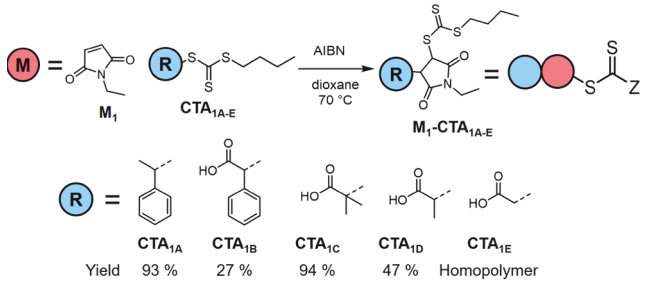

Figure 1. Various CTAs ($\mathbf{CTA_{1A-E}}$) were screened using *N*-ethyl maleimide ($\mathbf{M_1}$) under the same reaction conditions: $[M]_0$ = 1 M, $[CTA]_0$ = 1 M, $[AIBN]_0$ = 50 mM in dioxane at 70 °C for 4 h. From right to left monomer conversion (p) equals 0.98, 0.35, 0.97, 0.83, and 0.20 in the presence of respective CTAs and 0.98 without (See Figure S17 for detailed kinetics).

maleimides as slow homopropagating monomer is preferred to favor the chain transfer cycle.[27] We screened various R-groups that can be directly functionalized for tethering ($\mathbf{CTA_{1B}}$–$\mathbf{CTA_{1E}}$), using trithiocarbonate based CTA, since quantitative SUMI-CTA adduct yields of *N*-substituted maleimides have already been established with $\mathbf{CTA_{1A}}$.[21] Using *N*-ethyl maleimide as a model monomer ($\mathbf{M_1}$), under our reaction conditions, $\mathbf{CTA_{1A}}$ gave quantitative SUMI-CTA adduct yield (Figures S17 and S18 and Table S1); however, $\mathbf{CTA_{1B}}$, which only structurally differs from $\mathbf{CTA_{1A}}$ by an additional carboxylic acid, resulted in significantly slower kinetics (Figures S17 and S20 and Table S2). This was attributed to slower monomer addition from increased radical stability of the R• species contributed by the additional neighboring conjugation. Serendipitously, we found $\mathbf{CTA_{1C}}$, whose reactivity lies between the former two CTA's,[28] gave quantitative SUMI-CTA adduct yield (Figures S17 and S21 and Table S3). In contrast, $\mathbf{CTA_{1D}}$, with one less methyl substituent, resulted in significantly lower yield with unequal consumption of monomer and CTA (Figures S17 and S25 and Table S4). Furthermore, $\mathbf{CTA_{1E}}$, which does not favor chain transfer exchange with the monomer, resulted in retarded homopolymerization (Figures S17 and S27 and Table S5).[29]

As $\mathbf{M_1}$ and $\mathbf{CTA_{1C}}$ pairing demonstrates quantitative insertion yield, we synthesized **MCTA**, where the two functionalities are tethered together as the first AB type RAFT step-growth monomer. Herein, identical reaction conditions from the preliminary screening are used as the general procedure for RAFT step-growth polymerization. In all cases, we investigated the molecular weight evolution by conventional SEC analysis and ^{1}H NMR to determine the extent of the reaction (p). Interestingly, a downfield shift of the monomer end group was observed upon polymerization of **MCTA** (Figure 2A), and both the chain end "monomer" and unreacted monomers were considered to determine the overall p.

For linear step-growth polymerization, Flory has described theoretical molecular weight by number-average (M_n), weight-average (M_w), and Z-average (M_z), as a function of conversion, assuming no cyclization and equal end-group reactivity (details in Materials and Methods section S1.3).[30] Pleasingly, we found M_w and M_z trended with expected values (Figure 2B).[30] However, the low molecular weight cyclic species that are formed generally result in poorer agreement by M_n, which is commonly observed in other examples of step-growth polymerizations in the literature.[31] Typically, oligomeric cyclic species can be observed from ^{1}H NMR with a downfield shift relative to the polymer backbone (Figure 2A, Figure S31).[32]

It is important to note the loss of monomer functionality from external initiation (e.g., AIBN) is expected to reduce the overall molecular weight (Scheme S1). Generally, we found more reasonable agreement with theoretical average molecular weight by approximating imbalanced stoichiometry from initiation ($r_{th} = \left[\frac{1}{r} + 4f\frac{[I]_0}{[M]_0}(1 - e^{-k_d t})\right]^{-1}$, eq S9) (Table S7), which is subjective to the assumed value for initiation efficiency of the initiator[33] (details in Materials and Methods section S1.4). Here an initiation efficiency (f) of 0.65 is assumed as a constant value; however, it is important to note that the initiation efficiency typically falls at high monomer conversion.[33] Under our reaction conditions, high conversion was obtained after 4 h (p = 0.985) with 42% of the initiator theoretically consumed during the polymerization, leading to a r_{th} value of 0.949 and a theoretical M_w of 18k. However, leaving the reaction for longer time (18 h, Figure S36) would result in lower theoretical M_w, assuming the same initiation efficiency, as more initiator is consumed (Table S7).

Briefly examining reaction conditions with this AB monomer, we found the polymerization conducted at higher concentration is optimal for yielding higher molecular weight polymers with lower initiator equivalence (Figure S38 and Tables S8–S10). Interestingly, lowering the initial concentration of the polymerization resulted in more noticeable presence of the cyclic species (Figure 2C and Figure S39), which is a classical step-growth feature;[34] on the other hand, the rate followed pseudo-first-order kinetics that was dependent on initiator concentration (Figure S38).[35] Surprisingly, changing the solvent to DMSO or DMF had undesirable loss

https://doi.org/10.1021/jacs.1c07553
J. Am. Chem. Soc. 2021, 143, 15918–15923

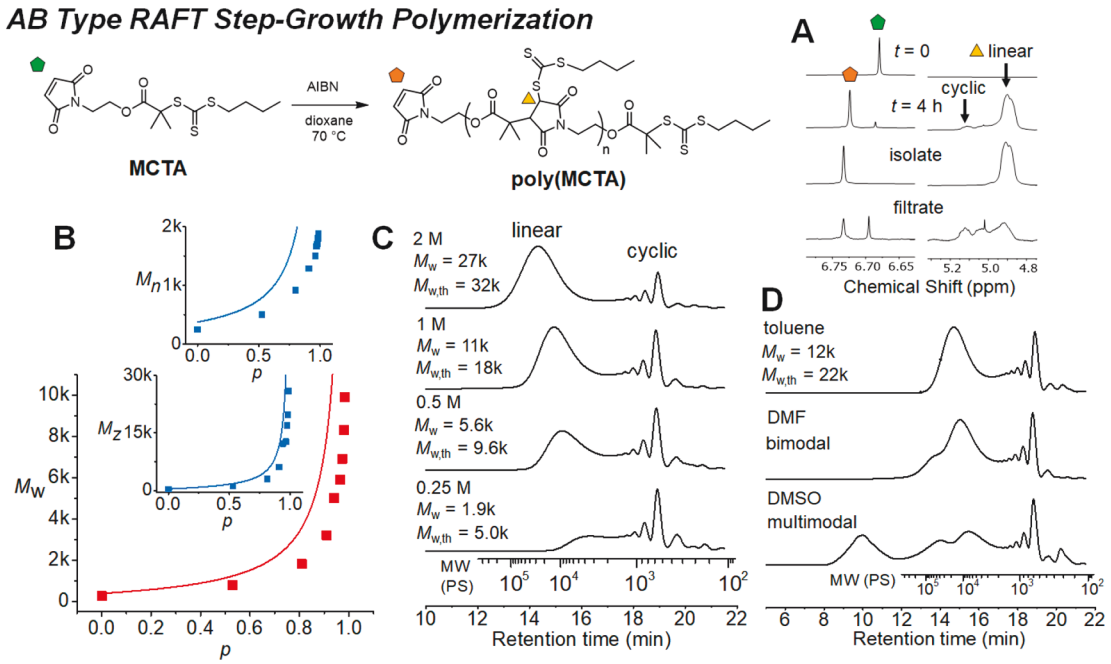

Figure 2. AB RAFT step-growth polymerization of **MCTA** using general conditions: $[\mathbf{MCTA}]_0$ = 1 M, $[\mathrm{AIBN}]_0$ = 50 mM in dioxane at 70 °C for 4 h. (A) ^{1}H NMR of initial monomer species and the polymer backbone at t = 0, 4 h, after precipitation and filtrate. (B) Experimental M_n, M_w, and M_z (from conventional SEC analysis, relative to polystyrene calibration in THF) versus monomer conversion, plotted together with expected values without considering imbalanced stoichiometry from initiation. SEC-dRI chromatograms of (C) polymerization carried out with different initial concentrations ($[\mathbf{MCTA}]_0$ = 2 to 0.25 M) with the same initiator concentration ($[\mathrm{AIBN}]_0$ = 50 mM) and (D) polymerization carried out in toluene, DMF, and DMSO. The theoretical M_{wth} considers initiator derived imbalanced stoichiometry.

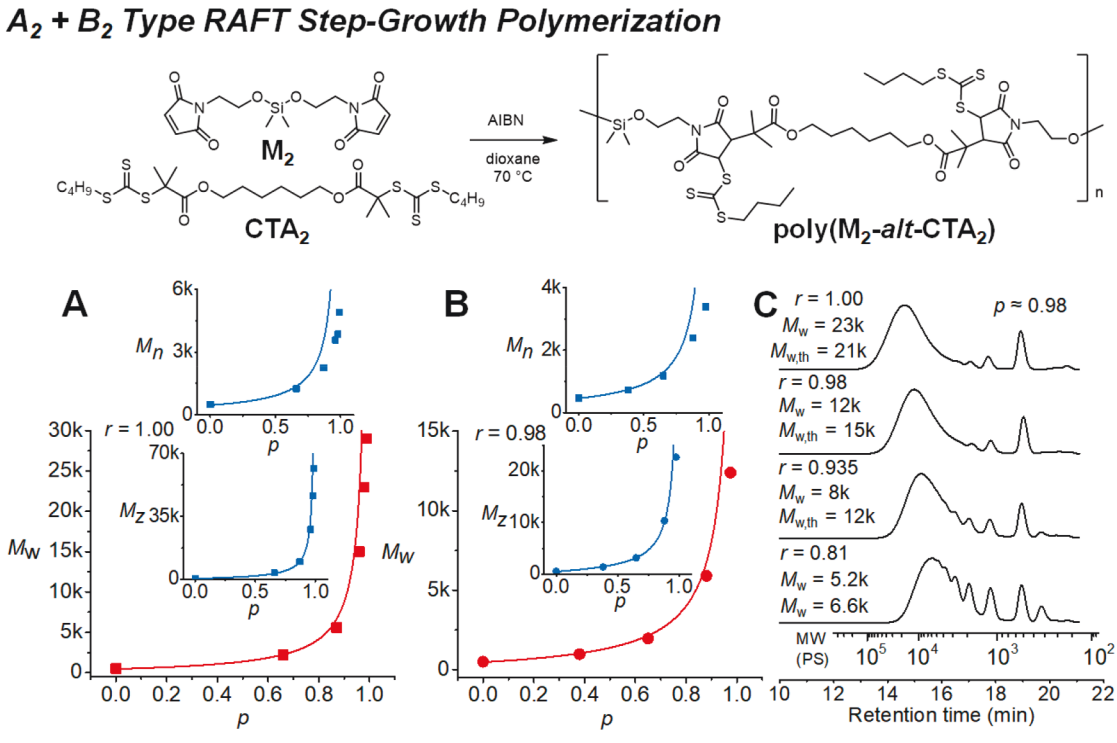

Figure 3. A_2 + B_2 RAFT step-growth of $\mathbf{M_2}$ and $\mathbf{CTA_2}$ using the general procedure $[\mathbf{M_2}]_0$ + $[\mathbf{CTA_2}]_0$ = 1.0 M, $[\mathrm{AIBN}]_0$ = 50 mM in dioxane at 70 °C for 4 h (r = $[\mathbf{M_2}]_0/[\mathbf{CTA_2}]_0$). Experimental M_n, M_w, and M_z versus monomer conversion plotted together with expected values using (A) equivalent (r = 1) and (B) nonequivalent stoichiometry (r = 0.98) of the two bifunctional reagents (without considering initiation). (C) Comparison of SEC-dRI chromatograms of the polymerizations (r = 1, 0.98, 0.94, 0.81) with approximately equal monomer conversion ($p \approx 0.98$) is presented (the theoretical M_{wth} considers initiator derived imbalanced stoichiometry).

of control, which was not observed using toluene or dioxane as the solvent (Figure 2D, Figure S41−42, and Table S11).

We next explored the RAFT step-growth polymerization with A_2 + B_2 type comonomers using bifunctional pairs of

https://doi.org/10.1021/jacs.1c07553
J. Am. Chem. Soc. 2021, 143, 15918−15923

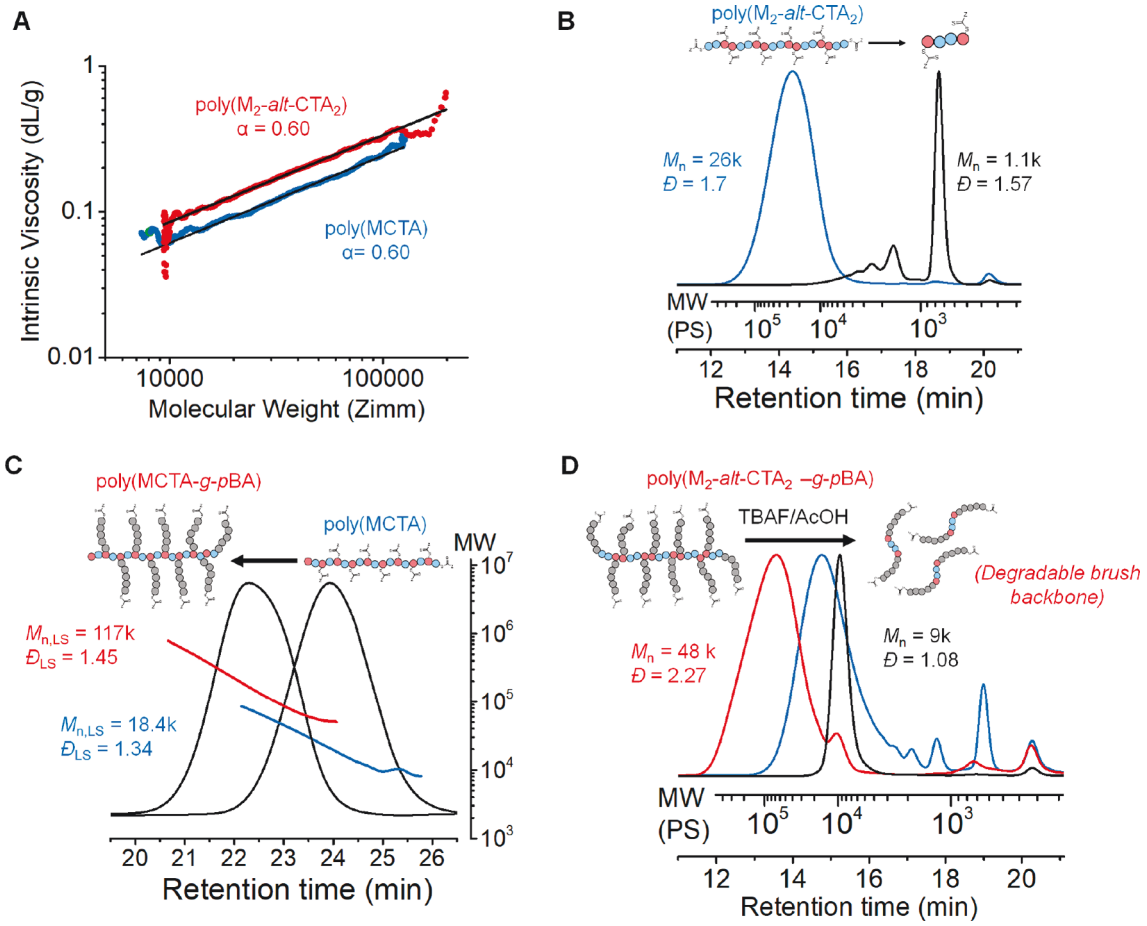

Figure 4. (A) Mark−Houwink plot of poly(M_2-*alt*-CTA_2) and poly(MCTA). (B) Degradation of isolated poly(M_2-*alt*-CTA_2) after 2 weeks under open atmospheric conditions. (C) SEC-dRI chromatograms of poly(MCTA-*g*-PBA_{15}) and its precursor backbone with molecular weight determined by light scattering (LS). (D) SEC-dRI chromatograms of poly(M_2-*alt*-CTA_2-*g*-PBA_{35}) (red trace) and its precursor backbone (blue trace). Black trace shows SEC analysis measured within 40 min after introducing 1:1 TBAF/AcOH (4 mM, 5 equiv w.r.t. Si−O bonds).

monomers ($\mathbf{M_2}$) and CTA ($\mathbf{CTA_2}$) (Figure 3), which was successfully achieved using the same general reaction conditions. Unlike the previous AB type step-growth (*vide supra*), downfield shift of the monomer end group was not observed during the polymerization (Figure S44). Remarkably, the effect of using excess $\mathbf{CTA_2}$ to imbalance the stoichiometry proceeded with expected reduction in molecular weight averages (Figure 3, Figures S45−47, and Table S12). In addition, compared to the AB type step-growth, lower fractions of cyclic species are expected to form as the probability of the chain ends to cyclize is reduced by a factor of 2,[36] resulting in better agreement of M_w and M_z/M_w with expected values (Table S12).

In all cases, the RAFT step-growth polymers were easily purifiable by simply precipitating the reaction mixture twice into diethyl ether to remove low molecular weight cyclic species (Figures 4B, 4C, S32, S35, S40, and S43). The collected supernatant from the precipitation shows upfield shifted broadened backbone CTA peaks (Figures 2A and S34) that were observed prior to precipitation, and the corresponding SEC analysis reveals discrete oligomeric cyclic species (Figure S35). Furthermore, typical Mark−Houwink plots by triple detection SEC (dRI, LS, VS) analysis (Figures S37 and S48) of the isolated polymers reveals an α value of 0.6, which is consistent with the molecular weight distribution of linear polymers (Figure 4A).[37]

Owing to the step-growth nature, specific functionality imbedded in the bifunctional reagents can be incorporated in the polymer backbone, such as dimethyl silyl ether in $\mathbf{M_2}$. Interestingly, we found this functionality to be particularly susceptible to hydrolysis,[38] and poly($\mathbf{M_2}$-*alt*-$\mathbf{CTA_2}$) was found to degrade when left under open atmospheric conditions (Figure 4B and Figures S49 and S50). It is important to highlight that such backbone degradability is a highly desirable feature for biomedical applications.[39,40]

Finally, we successfully synthesized molecular brush polymers from our RAFT step-growth backbone with poly(butyl acrylate) (*p*BA) side chains using conventional RAFT polymerization (Figure 4C and D). Over the years, numerous synthetic strategies of designing molecular brush polymers have emerged, due to their unique mechanical and colloidal properties;[41] however, there are limited methods that exist for tailoring the main chain backbone. We emphasize the ease of our methodology to prepare the polymer brushes that overcome these limitations. Indeed, poly($\mathbf{M_2}$-alt-$\mathbf{CTA_2}$-*g*-pBA_{35}) that bears cleavable silyl ether within each repeat unit along the length of the brush showed rapid stimuli-triggered degradation into well-defined linear polymers (M_n = 9,000, $Đ$ = 1.08) (Figure 4D), which was remarkably consistent with the expected molecular weight for two *p*BA chains ($M_{n,th}$ = 4,900 per side chain).

https://doi.org/10.1021/jacs.1c07553
J. Am. Chem. Soc. 2021, 143, 15918−15923

In summary, we demonstrate successful AB and A_2 + B_2 RAFT step-growth polymerization proceeding through the insertion process. This facile methodology allows designing backbone functional linear polymers and subsequently molecular polymer brushes after the second polymerization step, unlocking new opportunities for broad applications. We anticipate an expansion of RAFT step-growth polymerization with various monomers and tethering functional groups, owing to the modular nature of this polymerization and the robustness of RAFT agents.

■ ASSOCIATED CONTENT

Supporting Information

The Supporting Information is available free of charge at https://pubs.acs.org/doi/10.1021/jacs.1c07553.

Experimental details, materials and methods for synthesis and characterization. Equations and description of theoretical molecular weight averages (eqs S1−S6) and approximation of initiator derived imbalanced stoichiometry (eqs S7−S9). Additional scheme illustrating the initiation mechanism with AIBN (Scheme S1). NMR spectra of synthesized starting materials (Figures S1−S16). Tables and additional figures for characterization of RAFT-SUMI kinetic studies (Figures S17−S28 and Tables S1−S6), AB RAFT step-growth polymerization (Figures S29−S43 and Tables S7−S11), A_2 + B_2 RAFT step-growth polymerization (Figures S44−S48 and Table S12), degradation poly(M_2-*alt*-CTA_2) (Figures S49 and S50), and Mark−Houwink plot of poly(**MCTA**-*g*-*p*BA_{35}) (Figure S51). (PDF)

■ AUTHOR INFORMATION

Corresponding Authors

Joji Tanaka − *Department of Chemistry, University of North Carolina, Chapel Hill, North Carolina 27599, United States;* orcid.org/0000-0002-2134-8079; Email: joji@email.unc.edu

Wei You − *Department of Chemistry, University of North Carolina, Chapel Hill, North Carolina 27599, United States;* orcid.org/0000-0003-0354-1948; Email: wyou@unc.edu

Authors

Noel Edward Archer − *Department of Chemistry, University of North Carolina, Chapel Hill, North Carolina 27599, United States*

Michael Jeffery Grant − *Department of Chemistry, University of North Carolina, Chapel Hill, North Carolina 27599, United States*

Complete contact information is available at: https://pubs.acs.org/10.1021/jacs.1c07553

Notes

The authors declare the following competing financial interest(s): J.T. and W.Y. are named inventors on the provisional patent application described in this work.

■ ACKNOWLEDGMENTS

This work was financially supported by the National Science Foundation (NSF) under Award CHE-1808055. The Bruker AVANCE III Nanobay 400 MHz NMR spectrometer was supported by the National Science Foundation under Grant No. CHE-0922858. The authors thank Marc A. ter Horst and Andrew Camp from University of North Carolina Department of Chemistry NMR Core Laboratory for the use of their NMR spectrometers and Sue Mecham and Sally Lewis for THF-SEC instrumental training. Sergei Sheiko's guidance in preparing the manuscript and related discussion are specially acknowledged.

■ REFERENCES

(1) Gurnani, P.; Perrier, S. Controlled radical polymerization in dispersed systems for biological applications. *Prog. Polym. Sci.* **2020**, *102*, 101209.

(2) Corrigan, N.; Jung, K.; Moad, G.; Hawker, C. J.; Matyjaszewski, K.; Boyer, C. Reversible-deactivation radical polymerization (Controlled/living radical polymerization): From discovery to materials design and applications. *Prog. Polym. Sci.* **2020**, *111*, 101311.

(3) Chiefari, J.; Chong, Y. K.; Ercole, F.; Krstina, J.; Jeffery, J.; Le, T. P. T.; Mayadunne, R. T. A.; Meijs, G. F.; Moad, C. L.; Moad, G.; Rizzardo, E.; Thang, S. H. Living Free-Radical Polymerization by Reversible Addition−Fragmentation Chain Transfer: The RAFT Process. *Macromolecules* **1998**, *31* (16), 5559−5562.

(4) Perrier, S. 50th Anniversary Perspective: RAFT Polymerization—A User Guide. *Macromolecules* **2017**, *50* (19), 7433−7447.

(5) Moad, G.; Rizzardo, E.; Thang, S. H. Living Radical Polymerization by the RAFT Process − A Third Update. *Aust. J. Chem.* **2012**, *65* (8), 985−1076.

(6) Ikada, Y.; Tsuji, H. Biodegradable polyesters for medical and ecological applications. *Macromol. Rapid Commun.* **2000**, *21* (3), 117−132.

(7) Worch, J. C.; Dove, A. P. 100th Anniversary of Macromolecular Science Viewpoint: Toward Catalytic Chemical Recycling of Waste (and Future) Plastics. *ACS Macro Lett.* **2020**, *9* (11), 1494−1506.

(8) Rogers, M. E. L.; Timothy, E. *Synthetic methods in step-growth polymers*; John Wiley and Sons: New York, 2003.

(9) Keddie, D. J.; Moad, G.; Rizzardo, E.; Thang, S. H. RAFT Agent Design and Synthesis. *Macromolecules* **2012**, *45* (13), 5321−5342.

(10) Chong, Y. K.; Le, T. P. T.; Moad, G.; Rizzardo, E.; Thang, S. H. A More Versatile Route to Block Copolymers and Other Polymers of Complex Architecture by Living Radical Polymerization: The RAFT Process. *Macromolecules* **1999**, *32* (6), 2071−2074.

(11) Chong, Y. K.; Krstina, J.; Le, T. P. T.; Moad, G.; Postma, A.; Rizzardo, E.; Thang, S. H. Thiocarbonylthio Compounds [SC(Ph)S−R] in Free Radical Polymerization with Reversible Addition-Fragmentation Chain Transfer (RAFT Polymerization). Role of the Free-Radical Leaving Group (R). *Macromolecules* **2003**, *36* (7), 2256−2272.

(12) Chiefari, J.; Mayadunne, R. T. A.; Moad, C. L.; Moad, G.; Rizzardo, E.; Postma, A.; Thang, S. H. Thiocarbonylthio Compounds (SC(Z)S−R) in Free Radical Polymerization with Reversible Addition-Fragmentation Chain Transfer (RAFT Polymerization). Effect of the Activating Group Z. *Macromolecules* **2003**, *36* (7), 2273−2283.

(13) McLeary, J. B.; Calitz, F. M.; McKenzie, J. M.; Tonge, M. P.; Sanderson, R. D.; Klumperman, B. Beyond Inhibition: A 1H NMR Investigation of the Early Kinetics of RAFT-Mediated Polymerization with the Same Initiating and Leaving Groups. *Macromolecules* **2004**, *37* (7), 2383−2394.

(14) McLeary, J. B.; Tonge, M. P.; Klumperman, B. A Mechanistic Interpretation of Initialization Processes in RAFT-Mediated Polymerization. *Macromol. Rapid Commun.* **2006**, *27* (15), 1233−1240.

(15) McLeary, J. B.; Calitz, F. M.; McKenzie, J. M.; Tonge, M. P.; Sanderson, R. D.; Klumperman, B. A 1H NMR Investigation of Reversible Addition−Fragmentation Chain Transfer Polymerization Kinetics and Mechanisms. Initialization with Different Initiating and Leaving Groups. *Macromolecules* **2005**, *38* (8), 3151−3161.

(16) Houshyar, S.; Keddie, D. J.; Moad, G.; Mulder, R. J.; Saubern, S.; Tsanaktsidis, J. The scope for synthesis of macro-RAFT agents by sequential insertion of single monomer units. *Polym. Chem.* **2012**, *3* (7), 1879−1889.

(17) Zhou, Y.; Zhang, Z.; Reese, C. M.; Patton, D. L.; Xu, J.; Boyer, C.; Postma, A.; Moad, G. Selective and Rapid Light-Induced RAFT Single Unit Monomer Insertion in Aqueous Solution. *Macromol. Rapid Commun.* **2020**, *41* (1), 1900478.
(18) Aerts, A.; Lewis, R. W.; Zhou, Y.; Malic, N.; Moad, G.; Postma, A. Light-Induced RAFT Single Unit Monomer Insertion in Aqueous Solution—Toward Sequence-Controlled Polymers. *Macromol. Rapid Commun.* **2018**, *39* (19), 1800240.
(19) Quiclet-Sire, B.; Revol, G.; Zard, S. Z. A convergent, modular access to complex amines. *Tetrahedron* **2010**, *66* (33), 6656−6666.
(20) Liu, R.; Zhang, L.; Huang, Z.; Xu, J. Sequential and alternating RAFT single unit monomer insertion: model trimers as the guide for discrete oligomer synthesis. *Polym. Chem.* **2020**, *11* (28), 4557−4567.
(21) Huang, Z.; Corrigan, N.; Lin, S.; Boyer, C.; Xu, J. Upscaling single unit monomer insertion to synthesize discrete oligomers. *J. Polym. Sci., Part A: Polym. Chem.* **2019**, *57* (18), 1947−1955.
(22) Huang, Z.; Noble, B. B.; Corrigan, N.; Chu, Y.; Satoh, K.; Thomas, D. S.; Hawker, C. J.; Moad, G.; Kamigaito, M.; Coote, M. L.; Boyer, C.; Xu, J. Discrete and Stereospecific Oligomers Prepared by Sequential and Alternating Single Unit Monomer Insertion. *J. Am. Chem. Soc.* **2018**, *140* (41), 13392−13406.
(23) Xu, J.; Fu, C.; Shanmugam, S.; Hawker, C. J.; Moad, G.; Boyer, C. Synthesis of Discrete Oligomers by Sequential PET-RAFT Single-Unit Monomer Insertion. *Angew. Chem., Int. Ed.* **2017**, *56* (29), 8376−8383.
(24) Xu, J.; Shanmugam, S.; Fu, C.; Aguey-Zinsou, K.-F.; Boyer, C. Selective Photoactivation: From a Single Unit Monomer Insertion Reaction to Controlled Polymer Architectures. *J. Am. Chem. Soc.* **2016**, *138* (9), 3094−3106.
(25) Alfurhood, J. A.; Bachler, P. R.; Sumerlin, B. S. Hyperbranched polymers via RAFT self-condensing vinyl polymerization. *Polym. Chem.* **2016**, *7* (20), 3361−3369.
(26) Haven, J. J.; Hendrikx, M.; Junkers, T.; Leenaers, P. J.; Tsompanoglou, T.; Boyer, C.; Xu, J.; Postma, A.; Moad, G. Elements of RAFT Navigation. In *Reversible Deactivation Radical Polymerization: Mechanisms and Synthetic Methodologies*; American Chemical Society: 2018; Vol. *1284*, pp 77−103.
(27) Cramer, N. B.; Reddy, S. K.; O'Brien, A. K.; Bowman, C. N. Thiol−Ene Photopolymerization Mechanism and Rate Limiting Step Changes for Various Vinyl Functional Group Chemistries. *Macromolecules* **2003**, *36* (21), 7964−7969.
(28) Keddie, D. J. A guide to the synthesis of block copolymers using reversible-addition fragmentation chain transfer (RAFT) polymerization. *Chem. Soc. Rev.* **2014**, *43* (2), 496−505.
(29) Kwak, Y.; Goto, A.; Tsujii, Y.; Murata, Y.; Komatsu, K.; Fukuda, T. A Kinetic Study on the Rate Retardation in Radical Polymerization of Styrene with Addition−Fragmentation Chain Transfer. *Macromolecules* **2002**, *35* (8), 3026−3029.
(30) Flory, P. J. Molecular Size Distribution in Linear Condensation Polymers. *J. Am. Chem. Soc.* **1936**, *58*, 1877−1885.
(31) Estupiñán, D.; Gegenhuber, T.; Blinco, J. P.; Barner-Kowollik, C.; Barner, L. Self-Reporting Fluorescent Step-Growth RAFT Polymers Based on Nitrile Imine-Mediated Tetrazole-ene Cycloaddition Chemistry. *ACS Macro Lett.* **2017**, *6* (3), 229−234.
(32) Rosselgong, J.; Armes, S. P. Quantification of Intramolecular Cyclization in Branched Copolymers by 1H NMR Spectroscopy. *Macromolecules* **2012**, *45* (6), 2731−2737.
(33) Moad, G. A Critical Assessment of the Kinetics and Mechanism of Initiation of Radical Polymerization with Commercially Available Dialkyldiazene Initiators. *Prog. Polym. Sci.* **2019**, *88*, 130−188.
(34) Kricheldorf, H. R. The Role of Self-Dilution in Step-Growth Polymerizations. *Macromol. Rapid Commun.* **2008**, *29* (21), 1695−1704.
(35) Stenzel, M. H.; Barner-Kowollik, C. The living dead − common misconceptions about reversible deactivation radical polymerization. *Mater. Horiz.* **2016**, *3* (6), 471−477.
(36) Kricheldorf, H. R. Polycondensation of 'a − bn' or 'a2 + + bn' Monomers - A Comparison. *Macromol. Rapid Commun.* **2007**, *28* (18−19), 1839−1870.
(37) Lu, Y.; An, L.; Wang, Z.-G. Intrinsic Viscosity of Polymers: General Theory Based on a Partially Permeable Sphere Model. *Macromolecules* **2013**, *46* (14), 5731−5740.
(38) Parrott, M. C.; Luft, J. C.; Byrne, J. D.; Fain, J. H.; Napier, M. E.; DeSimone, J. M. Tunable Bifunctional Silyl Ether Cross-Linkers for the Design of Acid-Sensitive Biomaterials. *J. Am. Chem. Soc.* **2010**, *132* (50), 17928−17932.
(39) Shieh, P.; Nguyen, H. V. T.; Johnson, J. A. Tailored silyl ether monomers enable backbone-degradable polynorbornene-based linear, bottlebrush and star copolymers through ROMP. *Nat. Chem.* **2019**, *11* (12), 1124−1132.
(40) Delplace, V.; Nicolas, J. Degradable vinyl polymers for biomedical applications. *Nat. Chem.* **2015**, *7* (10), 771−784.
(41) Xie, G.; Martinez, M. R.; Olszewski, M.; Sheiko, S. S.; Matyjaszewski, K. Molecular Bottlebrushes as Novel Materials. *Biomacromolecules* **2019**, *20* (1), 27−54.

https://doi.org/10.1021/jacs.1c07553
J. Am. Chem. Soc. 2021, 143, 15918−15923